BEAMFORMING OF CIRCULAR MICROPHONE ARRAY WITH SOUND ABSORBENT CYLINDER

Ying Song and Susanto Rahardja

Institute for Infocomm Research, A*STAR, Singapore

ABSTRACT

Microphone array technology is an area which has generated a lot of interests in recent years. In this paper, a novel beamforming approach using microphone array mounted on the surface of a sound absorbent cylinder is discussed. By introducing of the sound absorbent cylinder with appropriate selected material acoustic characteristics, the "virtual aperture" of the circular array can

be enlarged thereby achieving the better beamforming performance. We first introduce an acoustic cylinder scattering model to provide a theoretical background. Subsequently, we derive the steering vector of the circular array outfitted with the sound absorbent cylinder based on the acoustic field model. The impact of the acoustic impedance to the beamforming accuracy is assessed. An acoustic impedance optimization criteria is developed to enhance beamforming performance. Numerical simulations are conducted to evaluate the theoretical results achieved.

Index Terms— acoustic signal processing, array signal processing, beamforming, DOA estimation.

1. INTRODUCTION

Microphone array technology has been studied extensively by both academic and industrial communities in recent years due to its widely diversified applications. Applications such as speech communication, teleconferencing, robot application and automation all require this technology [1]. Many types of microphone array structures have been proposed, including linear and circular arrays. However, circular arrays have wider applications due to their 360° beamforming capability.

Varieties of beamforming algorithms such as delay-and-sum [2], MVDR [3] and ESPRIT [4] have been developed. Among them, the delay-and-sum beamforming algorithm has been used widely, especially in robot navigation [5] and teleconferencing [6] due to advantages such as simple processing, robustness and suitability for the reverberation environment and simultaneous multiple sources application. The beamforming using circular array with cylinder have also been discussed recently. For example, Teutsch discussed mode beamforming with cylinder microphone array [7]. Zou proposed a cylinder vector sensor array mode beamforming algorithm [8] for underwater application. Gilles first presented the concept that a microphone array with cylinder gives the array an effectively larger aperture by numerical example, although he did not give a derivation of the matching steering vector [9].

In this paper the acoustic cylinder scattering model is introduced in Section 2. In the model, the sound field is contributed by both incident and scattering sound wave. The delay-and-sum beamforming with sound absorbent cylinder is presented and the matching steering vector is derived in Section 3. An approach to choose optimum cylinder acoustic impedance based on optimum directional index criterion of beamforming is proposed in Section 4. In Section 5 numerical simulations are conducted to evaluate the theoretical results. We conclude our findings and results in Section 6.

2. PHYSICAL MODEL OF CIRCULAR AIR VECTOR SENSOR

Consider a plane sound wave which incidents on a cylinder shown in Figure 1. The cylinder is positioned vertically at the origin of the Cartesian coordinate system. The axis of the cylinder is taken as the z-axis. Let the air density and sound velocity of the air be represented by ρ and c, respectively. The cylinder of radius $r = a$ is made of sound absorbent material with normal acoustic impedance of Z. The following relationship exists between the surrounding air density and sound velocity [11] .

$$Z = \frac{\rho c}{\gamma - j\sigma}, \tag{1}$$

where $j^2 = -1$ and γ and σ are the specific conductance and specific susceptance [12], respectively. Let the unit-magnitude of the

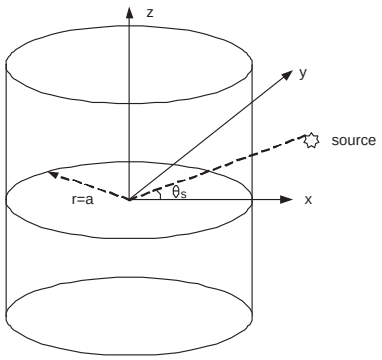

Fig. 1. Geometry of the cylinder.

steady state plane acoustic wave with radial frequency ω travelling in the direction of azimuth angle be θ_s and elevation angle be ϕ_s, respectively. Without loss of generality, we assume $\phi_s = \pi/2$. This can be justified easily when the acoustic source is far away from the array. The acoustic pressure of the incident wave around cylinder can be written as [9], [11]

$$p_i = \sum_{n=0}^{\infty} (-j)^n \epsilon_n J_n(kr) \cos[n(\theta - \theta_s)] e^{-j\omega t}, \tag{2}$$

where r is the distance from the observation point to the origin point of the coordinate system, $k = \omega/c$ is the wave number in air, $J_n(\cdot)$ is

 ISSN 2076-1465

the nth order Bessel function of the first kind, and ϵ_n is the Neumann function

$$\epsilon_n = \begin{cases} 1 & n = 0 \\ 2 & n = 1, 2, 3... \end{cases}$$

Similarly, the pressure caused by the scattering wave around cylinder can be written as [10][11]

$$p_s = \sum_{n=0}^{\infty} b_n H_n^{(1)}(kr) \cos[n(\theta - \theta_s)] e^{-j\omega t}, \tag{3}$$

where $H_n^{(1)}(\cdot)$ is the Hankel function of the first kind. The b_n is the reflection coefficient which is determined by the boundary conditions[12]. b_n can be derived as:

$$b_n = -\frac{(-j)^n \epsilon_n [\frac{Z}{\rho c} J_n'(kr) + j J_n(kr)]}{\frac{Z}{\rho c} H_n'^{(1)}(kr) + j H_n^{(1)}(kr)}. \tag{4}$$

The total sound field due to both incident and scattered wave is

$$\begin{aligned} p_T =& p_i + p_s \\ =& \sum_{n=0}^{\infty} [(-j)^n \epsilon_n J_n(kr) + b_n H_n^{(1)}(kr)] \\ & \cos[n(\theta - \theta_s)] e^{-j\omega t}. \end{aligned} \tag{5}$$

3. BEAMFORMING WITH SOUND ABSORBENT CYLINDER

Under the conventional far-field assumption, to assume a source at azimuthal angle θ_s, the array output vector takes the form [3]:

$$\boldsymbol{x}(t, \theta_s) = \boldsymbol{g}(\theta_s) s(t) + \boldsymbol{u}(t), \tag{6}$$

where $s(t)$ is the original source signal, $\boldsymbol{u}(t)$ is the additional noise, $\boldsymbol{g}(\theta_s)$ is the array steering vector. The output vector and steering vector of an array with M sensors can be represented as:

$$\boldsymbol{x}(t) = [x_1(t, \theta_s) \quad \cdots x_m(t, \theta_s) \quad \cdots x_M(t, \theta_s)]^T \tag{7}$$

and

$$\boldsymbol{g}(\theta_s) = [g_1(\theta_s) \quad \cdots g_m(\theta_s) \quad \cdots g_M(\theta_s)]^T, \tag{8}$$

respectively. The array response is steered by forming a linear combination of the sensor output which is defined as:

$$y(t) = \sum_{m=1}^{M} w_m^* x_m(t) = \boldsymbol{w}^H \boldsymbol{x}(t), \tag{9}$$

where $\boldsymbol{w}$ is weighting vector and $(.)^H$ denotes Hermitian transpose. Given snapshots $y(1)$, $y(2)$,...,$y(L)$, the output power is measured by

$$P = \boldsymbol{w}^H \hat{\boldsymbol{R}} \boldsymbol{w}, \tag{10}$$

where $\hat{\boldsymbol{R}}$ is the estimation of the covariance matrix $\boldsymbol{R}$ which is defined as:

$$\boldsymbol{R} = E[\boldsymbol{x}(t) \boldsymbol{x}^H(t)]. \tag{11}$$

Given L temporal samples $x(t_0), x_(t_1), .. ., x(t_{L-1})$, the value of $\hat{\boldsymbol{R}}$ can be estimated as

$$\hat{\boldsymbol{R}} = \frac{1}{L} \sum_{l=0}^{L-1} \boldsymbol{x}(t_l) \boldsymbol{x}^H(t_l). \tag{12}$$

When the assumption of spatially white noise is applied, the weighting vector and array output spectrum for delay and sum beamforming can be derived as

$$\boldsymbol{w}(\theta_s) = \frac{\boldsymbol{g}(\theta_s)}{\sqrt{\boldsymbol{g}^H(\theta_s) \boldsymbol{g}(\theta_s)}} \tag{13}$$

and

$$P(\theta_s) = \frac{\boldsymbol{g}^H(\theta_s) \hat{\boldsymbol{R}} \boldsymbol{g}(\theta_s)}{\boldsymbol{g}^H(\theta_s) \boldsymbol{g}(\theta_s)}, \tag{14}$$

respectively. For the circular microphone array with M sensors without cylinder, the mth sensor output without noise is only composed of the incident wave. It can be formed as

$$x_{i_m}(t) = p_i(\theta_m, t). \tag{15}$$

The steering vector actually presents the phase and the amplitude difference between the first sensor and the rest of the sensors. It presents as:

$$g_{i_m}(\theta_s) = e^{-jka\cos(\theta_m - \theta_s)}. \tag{16}$$

When a circular array mounted around the perimeter of the sound absorbent cylinder, without noise assumption, at time t, the mth sensor senses both the incident and scattering acoustic field which can be represented as

$$x_{T_m}(t) = p_T(\theta_m, t) = p_i(\theta_m, t)(1 + \frac{p_s(\theta_m, t)}{p_i(\theta_m, t)}). \tag{17}$$

Equation (17) can be further denoted as

$$x_{T_m}(t) = p_i(\theta_m, t)(1 + f_m(\theta_s)), \tag{18}$$

where f_m is the mth correcting factor, it can be obtained:

$$f_m(\theta_s) = \frac{\sum_{n=0}^{\infty} b_n H_n^{(1)}(kr) \cos[n(\theta_m - \theta_s)]}{\sum_{n=0}^{\infty} (-j)^n \epsilon_n J_n(kr) \cos[n(\theta_m - \theta_s)]}. \tag{19}$$

Comparing with equations (15) and (18), it can be found that extra phase and amplitude distortion are introduced by the scattering field. We introduce a new steering vector to factor in this phase and amplitude distortion as

$$g_{T_m}(\theta_s) = e^{-jka\cos(\theta_m - \theta_s)}(1 + f_m(\theta_s)), \tag{20}$$

and the spatial wavenumber spectrum as

$$P(\theta_s) = \frac{\boldsymbol{g}_T^H(\theta_s) \hat{\boldsymbol{R}}_T \boldsymbol{g}_T(\theta_s)}{\boldsymbol{g}_T^H(\theta_s) \boldsymbol{g}_T(\theta_s)}. \tag{21}$$

where $\hat{\boldsymbol{R}}_T$ is derived by replacing $\boldsymbol{x}$ with $\boldsymbol{x}_T$ in equation (12).

4. DERIVATION OF OPTIMUM ACOUSTIC IMPEDANCE

In Section 3, we have shown that the spatial spectrum of beamforming is a function of impedance given a dedicated array architecture of array size, sensor number, position and central frequency as shown in equation (21). It is difficult to derive a close-form solution for beamforming optimization with respect to acoustic impedance Z. Instead, numerical analysis is used to solve the problem.

The performance of beamforming can be evaluated by varieties of parameters. Among them the 3dB beamwidth, mainlobe to sidelobe ratio (maximum sidelobe level) are the most important specifications. The 3dB beamwidth is the parameter to evaluate the spatial resolution. Maximum sidelobe level is used to evaluate the noise

suppression capability. Let $F_{t_{bw}}(Z)$ denote the 3dB beamwidth with respect to acoustic impedance, the optimized 3dB beamwidth can be presented as

$$F_{t_{bw}}(Z_{bw_o}) = \min\{F_{t_{bw}}(Z)\}. \quad (22)$$

Similarly, F_{t_s} is the optimized sidelobe with respect to impedance which can be denoted as

$$F_{t_s}(Z_{s_o}) = \min\{F_{t_s}(Z)\}. \quad (23)$$

Ideally, it can be optimized when $Z_{bw_o} = Z_{s_o}$. However, it may not be always the case in practical situation. Sometimes optimized sidelobe is related to poor 3dB beamwidth performance and vice versa. To balance the beamforming performance the Directivity Index (DI) is selected. The DI gives a summary evaluation for the beam pattern which is defined as:

$$DI = 10log_{10}(P(\theta_s)) - 10log_{10}(\frac{\sum_{\theta=0}^{2\pi} P(\theta)}{2\pi}). \quad (24)$$

The DI is a balanced optimization parameter comparing with the 3dB beamwidth and maximum sidelobe. The bigger DI denotes the overall better beamforming performance. The maximization of DI

$$DI(Z_{opt}) = \max\{DI(Z)\} \quad (25)$$

can be achieved by numerical analysis. The overall beamforming performance is optimized when Z_{opt} is reached.

5. NUMERICAL EXAMPLES AND DISCUSSION

In this section, we evaluate some of the theoretical analysis proposed in Sections 3 and 4 by numerical examples. The related simulation parameters are shown in Table.1.

Figures 2 and 3 simulate the optimization of the directional index with respect to acoustic impedance at $f = 660$Hz and 1320Hz respectively. Coarse search shows that the impedance impacts the DI most significantly at magnitudes ranging from $10^{-2}\rho c$ to ρc and phase ranging from 0 to π in radian . Exhaustive search with magnitude resolution of $\frac{3}{40}$ in logarithm scale from $10^{-2}\rho c$ to $10^{1}\rho c$ and a phase resolution of $\frac{\pi}{60}$ from 0 to 2π radian are adopted for the computation. All the local maximums are detected with peak detection algorithms and the global maximum is identified by comparing the magnitude of all the maximum. It is observed from Figure 2, for $f = 660$Hz, the maximum DI of 9.53dB is detected at impedance magnitude index 23 and impedance phase index 32, which corresponds to the impedance magnitude $0.4924\rho c$ and phase 1.6368 radian. Similarly, from Figure 3 at $f = 1320$Hz, the optimized impedance is at impedance magnitude index 24 and impedance phase index 31, which corresponds to the impedance $Z_{opt} = 0.5878e^{1.584j}\rho c$ and that leads a maximized DI of 11.23dB.

The sensor arrays under assessment include circular microphone array without cylinder, circular microphone array with un-optimized impedance of $Z_0 = (2 - \frac{j36}{13ka})\rho c$ and circular array with optimized cylinder impedance which is derived using approach proposed in Section 4. For easy presentation, we denote normal uniformed circular microphone array as use "Case 1". We use "Case 2" and "Case 3" to denote microphone array with Z_0 impedance cylinder and array with optimized impedance cylinder, respectively.

Simulation Parameters	
Air density	$1.2 \times 10^{-5}\ kg/m^3$
Sound speed in air	343 m/sec
Sensor number	16
Cylinder radius	0.133 m
Sampling rate	$8kHz$
Window length	32000

Table 1. Simulation parameters.

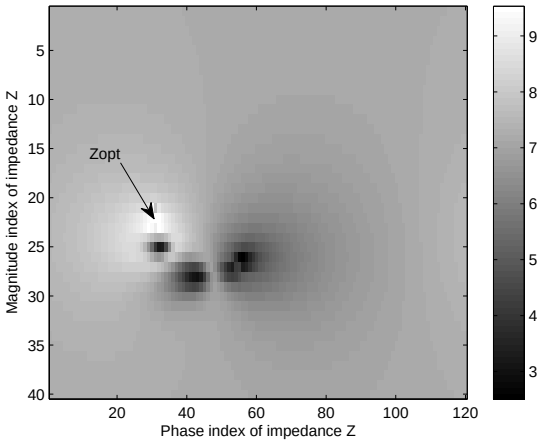

Fig. 2. Performance Index at f=660Hz

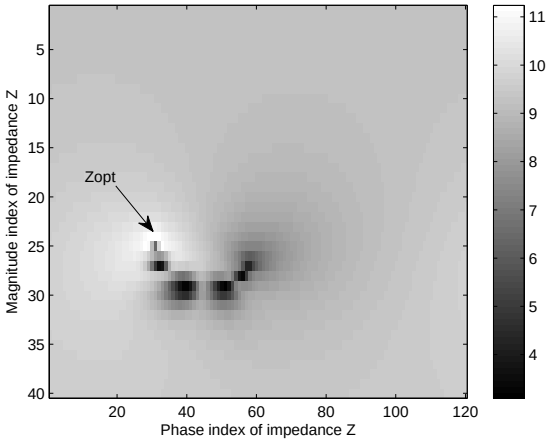

Fig. 3. Performance Index at f=1320Hz

Assuming there is a far-field acoustic source emanating sound wave to the array with azimuth angle of 0°. Without loss of generality, we adopt the following parameters for our simulations shown in Table 1.

The simulation results of beamforming of the three types of array at $f = 660$Hz are shown in Figure 4. It is observed that under the same array geometry, the optimized angle 3dB beamwidth is $\pm 16^\circ$ with the optimized impedance value for Case 3, a significant improvement comparing with $\pm 41^\circ$ for Case 1 and $\pm 33^\circ$ for Case 2, respectively. Slight sidelobe reduction is compared to Case 3 with maximum sidelobe level of -11dB, comparing with -10dB for Case 1.

Figure 5 shows the second simulation example of beamforming with three types of array at 1320Hz. Compared with Figure 4,

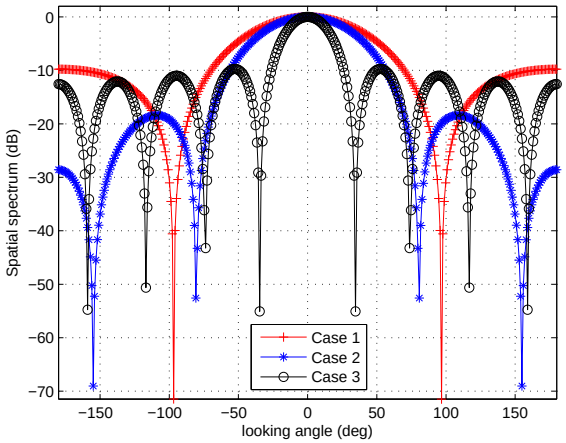

Fig. 4. Beam pattern at f=660Hz

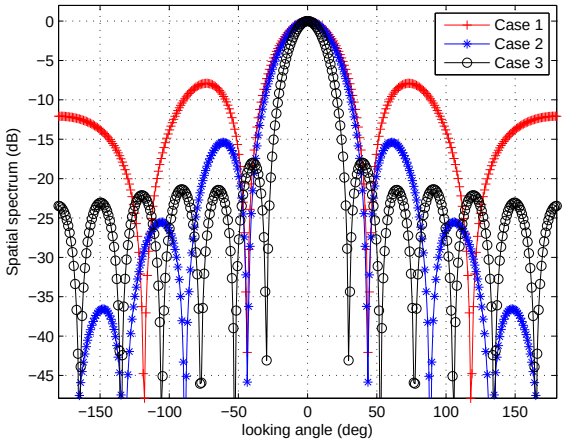

Fig. 5. Beam pattern at f=1320Hz

similar improvements are observed though the 3dB beamwidth improvement is less significant. The maximum sidelobe level for Case 3 is -18dB, which is 10dB and 3.4dB lower than Case 1 and Case 2 respectively.

We observed from both simulation examples that the beamwidth is narrowed to by introducing the sound absorbent cylinder which is equivalent to an enlargement of the array aperture. We address this as "virtual array" enlargement. As the frequency increases the "virtual aperture" enlargement effect is weakened even with the optimized impedance.

6. CONCLUSION

In this paper, we discuss a novel beamforming approach using microphone array mounted on the surface of a sound absorbent cylinder. By using of the sound absorbent cylinder with appropriate selected material acoustic characteristics, the "virtual aperture" of the circular array can be enlarged and beamforming performance can be significantly improved. An acoustic cylinder scattering model is first introduced to provide a theoretical background. The steering vector of the circular array outfitted with the sound absorbent cylinder based upon the acoustic field model is subsequently derived. An acoustic impedance optimization criteria is developed to enhance beamforming performance. Finally, numerical simulations are conducted to evaluate the theoretical results achieved.

We propose a directional index optimization criteria whichis a trade-off of bandwidth and maximum sidelobe optimization. As the close-form solution could be tedious, numerical solution is selected to search the optimized impedance. The approach can be used for array design optimization. If the array designer demands special emphasis on any dedicated parameters, new criteria can be defined for impedance optimization.

7. REFERENCES

[1] Yiteng (Arden) Huang and Jacob Benesty, *Audio signal processing for next-generation multimedia communication systems*, Kluwer Academic Publishers, Boston, 2004.

[2] H. Krim, M. Viberg, "Two decades of array signal processing research, the parametric approach," *IEEE Signal Processing Magazine*, pp. 67-94, July 1996.

[3] J. Capon, "High-Resolution Frequency-Wavenumber Spectrum Analysis," *Proc. IEEE*, 57(8):2408-1418, Aug. 1969.

[4] R. Roy and T. Kailath, "ESPRIT - estimation of signal parameters via rotational invariance techniques, *IEEE Trans. Acoust, Speech and Signal Processing* , vol. 37, no. 7, pp. 984-995, July. 1989.

[5] Yuki.Tamai, Yoshimichi Ito and Nobora Babaguchi, "Audio based estimation of speakers directions for multimedia meeting logs," *Proc. IEEE ICME*, pp. 212-215, 2007.

[6] Yuki.Yokoe, Satoshi Kagami, Yutaka Amemiya, Yoko Sasaki, Hiroshi Mizoguchi and Tachio Takano, "Circular microphone array for robot's audition," *Proc. IEEE Sensors*, pp. 565-570, 2004.

[7] H.Teutsch and W. Kellermann, "EB-ESPRIT: 2D localization of multiple wideband acoustic sources using eigen-beam," *Proc. IEEE ICASSP*, vol.3, pp. 89-92, 2005.

[8] N. Zou and A.Nehorai, "Circular acoustic vector-sensor array for mode beamforming ," *IEEE Trans. signal Processing*, vol. 57, no. 8, pp. 3041-3052, Aug. 2009.

[9] G. A. Daigle, Michael R. Stinson, and James G. Ryan, "Beamforming with air-coupled surface waves around a sphere and circular cylinder," *Journal of Acoustic Society of America*, vol. 117, no. 6, pp. 3373-3376, June. 2005.

[10] M. Lax and H. Feshbach, "Absorption and scattering for impedance boundary conditions on spheres and circular cylinders," *Journal of Acoustic Society of America*, vol. 20, no. 2, pp. 108-124, Mar. 1948,

[11] R. K. Cook and P. Chrzanowski, "Absorption and scattering by sound absorbent cylinders"*Journal of Acoustic Society of America*, vol. 17, no. 4, pp. 315-325, Apr. 1946.

[12] D. A. James, "Acoustic scattering from a semi-infinite, elastic, cylindrical shell," *Journal of Sound and Vibration*, vol. 196, no. 2, pp. 203-236, 1996.